ELSEVIER

International Journal of Mass Spectrometry 216 (2002) 269–284

International Journal of Mass Spectrometry

www.elsevier.com/locate/ijms

Measurement of external ion injection and trapping efficiency in the ion trap mass spectrometer and comparison with a predictive model

A.D. Appelhans*, D.A. Dahl[1]

Idaho National Engineering and Environmental Laboratory, P.O. Box 1625, Idaho Falls, ID 83415-2208, USA

Received 22 October 2001; accepted 8 March 2002

Abstract

The efficiency of injecting and trapping ions from an external ion source in a quadrupole ion trap mass spectrometer was measured and compared against a simulation employing a simple hard-sphere collision model. A commercial ion trap mass spectrometer was modified with the addition of a variable energy ion gun, split Faraday cup/electron multiplier detector, and the capability to measure the ion current incident on the ion trap inlet and exit end caps. The entire instrument was modeled using the ion optics simulation program SIMION and user programs were applied in SIMION which modeled the collisions between the injected ions and the helium buffer gas. The model was based on simple hard-sphere collision physics with randomized collision angles and collision probability converging to the mean free path (mfp); the helium buffer gas was assumed to be at rest relative to the injected ions. The measured trapping efficiency of Cs^+ with helium buffer gas at optimum conditions was 3–5%. The trapping efficiency predicted by the model and the dependence on buffer gas pressure (mfp) agreed with the measured efficiencies within the uncertainties of the model predictions and experimental variance. The fidelity of the simulation was shown to be sensitive to the spatial resolution of the model when predicting the dependence of trapping efficiency on q_z. It was concluded that a hard-sphere collision model was adequate for predicting the effects of helium buffer gas pressure on ion injection and trapping within the range of injection energies and buffer gas pressures tested. (Int J Mass Spectrom 216 (2002) 269–284) © 2002 Elsevier Science B.V. All rights reserved.

Keywords: Quadrupole ion trap; Ion injection; Secondary ion mass spectrometry (SIMS); Simulation; SIMION

1. Introduction

Application of the quadrupole ion trap mass spectrometer beyond its routine use in gas chromatography mass spectrometry (GCMS) has inspired study of the processes controlling the injection of ions into the ion trap and their subsequent trapping within the rf field. Within the broad category of external ion injection, the studies to date can be divided between pulsed ion sources, such as laser desorption [1] and MALDI [2,3] and continuous ion sources such as electron impact [4–6] electrospray [7], glow discharge [8], and secondary ion mass spectrometry (SIMS) [9]. More specifically, for continued development of the ion trap mass spectrometer for use in SIMS, there is a need for a predictive model for investigating the effects of the ion insertion optics and the end cap geometry (hole size and grid arrangements). Quarmby and Yost [7] presented a detailed study of the injection and

* Corresponding author. E-mail: ada2@inel.gov
[1] Retired.

1387-3806/02/$ – see front matter
PII S1387-3806(02)00627-9

trapping of ions from an electrospray source along with simulations that illuminated many of the issues relative to injection and trapping and that highlighted the importance of a simulation model that implicitly accounted for aberrations in the end cap geometry (the presence of holes). Their results confirmed and illuminated previously noted effects [4,10] of the rf phasing and q_z on the trapping efficiency, the role that the helium buffer gas plays in trapping, and the energy- and mass-dependence of trapping efficiency. However, the absolute trapping efficiency was determined only via the model results, while the experimental measurements provided a qualitative measure of the relative trapping efficiency as a function of the various parameters (energy, buffer gas pressure, mass, etc.). Qin and Chait [2] measured absolute trapping efficiencies for large peptides produced via MALDI, but did not utilize a predictive model. Doroshenko and Cotter [3] measured trapping efficiencies for MALDI-produced ions in which a ramped rf was applied during ion injection. They showed that by appropriate synchronization of the injected ion pulse with the phase and amplitude of the rf level, that very high trapping efficiencies could be attained. Unfortunately, this technique requires very short pulses of ions (150 μs or less) and is not applicable to continuous beam injection. Weil et al. [11] showed with simulations that trapping efficiency was <5% for continuous injection but could be increased using short injection pulses combined with a bi-polar dc pulse applied to the end cap during trapping, but these results were not demonstrated experimentally. Kofel [4] measured an integrated injection/trapping/detection efficiency but did not compare the results against a model. Wells et al. [12] utilized a collision model based on a combination of hard-sphere and Langevin collision cross-sections in their study of chemical mass shifts, but did not apply the model to trapping of injected ions. He and Lubman [13] simulated external ion injection and applied a three-dimensional collision model, but did not compare the predictions with experiment.

Over the years, we had applied a simple three-dimensional hard-sphere collision model coupled with a conventional mean free path (mfp) calculation in studying the trapping of injected ions and designing various ion optical components. The model appeared to provide results that were qualitatively consistent with experimental results; however, the quantitative fidelity of the model was unknown. Thus, the goal in this current study was to perform absolute ion transport and trapping efficiency measurements for conditions typical for injection of ions produced by particle desorption (SIMS), and evaluate the quantitative performance of the model in simulating the experimental system. An experimental system was constructed to enable controlled injection of a homogeneous beam of elemental ions at controlled energy with a narrow energy distribution into the ion trap and to measure the injected current and the number of ions trapped at various pressures. The SIMION [14] ion optics program was used as the base of the predictive model. A set of user programs was developed for simulating collisions between the injected ions and the buffer gas; controlling randomization of the ion parameters, collision parameters, and rf phasing; setting the q_z value and other trap parameters; and logging the data. The model included the entire experimental system from ion source to detector. Experiments and simulations were performed at the same conditions and the fidelity of the simulations was assessed against the experiments.

2. Experimental

2.1. Physical system

The experimental system, illustrated in Fig. 1, included an ion trap modified to permit measurement of the ion current impinging on the inlet and exit end caps, a split detector system incorporating a Faraday cup and an electron multiplier, an ion gun capable of producing ions with kinetic energy from 3 to 5000 eV, a Cs^+ ion source producing a beam of >99% pure Cs^+, and a simple set of ion optic elements for guiding the beam into the aperture in the inlet end cap. The ion trap mass spectrometer is a modified Teledyne Discovery 2 (Teledyne, Mountain View, CA) system

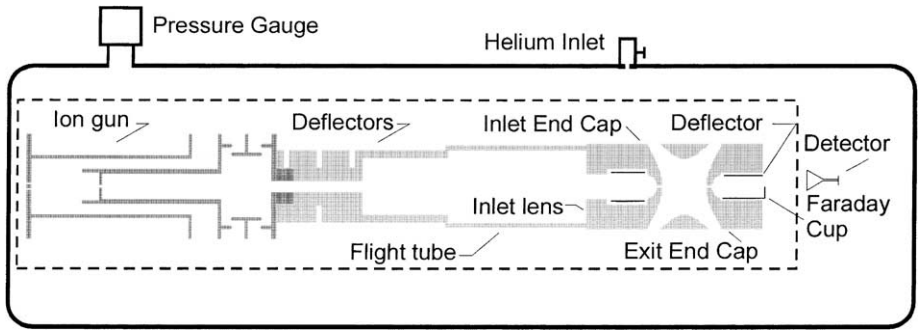

Fig. 1. Modified quadrupole ion trap mass spectrometer showing the location of the helium buffer gas inlet and the pressure gauge relative to the beam line and ion trap in the vacuum housing. Components inside the dashed area were included in the simulation.

with conventional ion trap dimensions ($r_o = 1$ cm, $r_z = 0.783$ cm) typical of the stretched configuration [15]. The detector system was modified to include a Faraday cup mounted within the exit end cap. A deflection electrode mounted opposite the Faraday cup was used to direct the ions ejected from the ion trap either into the Faraday cup or into the electron multiplier detector, located just outside of the exit end cap. Both the inlet and exit end caps could be connected to an electrometer to measure the ion current impinging on them, and the exit end cap could be coupled into the Faraday cup to measure total ion current injected into the trap. The Faraday cup was also used to calibrate the electron multiplier gain and linearity. Current measurements were made with Keithley model 617 electrometers (Keithley Instruments, Cleveland, OH). To determine if the ions caused secondary electron emissions (which would appear as a positive current), or if the positive ions were able to rebound off the surface (and not be counted), the end cap and Faraday cup were biased at +9 and −9 V for selected measurements. The measurements showed that a bias was not required (not unexpected given the low ion energies), and so measurements were made via direct connection of the end cap and Faraday cup to the electrometer. The trapped ions were ejected using axial modulation resonance ejection and measured using the electron multiplier connected to the Teledyne data system.

The ion source was a Cs^+ zeolite material heated to ∼800 °C which produced a 5–100 pA beam of >99% Cs^+ ions with no mass filtering. The ion gun was developed in our laboratory [16] and can produce a beam of ions with kinetic energy ranging from 3 to 5000 eV. The ion gun was coupled to the ion trap via two sets of deflectors [17] and a short flight tube. The flight tube was included to provide a well-defined and controlled electrostatic path for the ion beam as it travelled from the ion gun to the ion trap. The potential of the ion gun, beam deflectors, and the flight tube could be floated above the ground. This allowed the ion beam to be formed and transported at higher energy (∼100 eV) which reduced the diverging effects of the helium collision gas through this region. The ions were decelerated to the desired injection energy using the inlet lens located in front of the inlet end cap. This configuration allowed the ion injection flux to be held relatively constant over a wide range of energies. A second set of deflectors was located within the inlet end cap and provided final adjustment of the beam position and lensing for changing the beam shape at the inlet aperture. The ion gun and other electronics were controlled through a separate pulse control module that was triggered from the Teledyne data system.

System pressure was measured with a Varian Eyesys Mini-BA (Varian Vacuum Technologies, Corp.) mini-ion-gauge that was calibrated against a full-sized Bayard-Alpert gauge (Varian Corp., model 571) and a Baratron (MKS Corp., model 627B). All pressure references in the text are the measured gauge pressure uncorrected for gas composition, while all mfps

were calculated based on the calibrated gauge pressure corrected for gas composition. Collision gas was admitted directly into the vacuum housing ∼5 cm from the ion trap and measured at a point ∼15 cm from the gas inlet. The end cap-to-ring spacers had multiple openings to ensure that the pressure inside the ion trap would be the same as the total system pressure. The collision gas pressure was assumed uniform throughout the vacuum housing and within the ion trap and ion gun assemblies.

3. Analytical and numerical models

The SIMION ion optics simulation program was used to model the physical experiment and a collision model was incorporated in a user program within the SIMION model. The entire physical instrument used in the experiment was modeled in order to investigate all the effects of collisions along the beam line (such as reduction in kinetic energy via collisions) and the effects these might have on ion injection.

3.1. SIMION geometry model

Fig. 1 shows the full system model as used in SIMION. Ions originated at the ion source, and the voltages used in the experiments were used in the model for assessing performance. For the full-system simulation, five separate array instances were used in order to accommodate the asymmetric nature of the ion optical elements. The initial scale factor used for the ion trap was 0.5 mm/grid-unit (gu), and the scale factor was later refined to 0.0625 mm/gu. Fig. 2 shows a cross-section of the ion trap and inlet lens portion of the system with a set of ion trajectories for ions with 12 eV of kinetic energy, along with a *y*-expanded view of the trajectories. Note that the ion beam is tightly focused, that the ions are entering the ion trap with a very low divergence angle, and that the majority of the ions pass through the exit end cap aperture. The trajectories illustrated in Fig. 2 were calculated with mfp of 1200 cm, and thus, there were essentially no collisions occurring. The higher resolution model of the ion trap was used to study the injection-dependence on q_z and the trapping efficiency (discussed in Section 4). The ion trap model was based on the as-built dimensions of the Teledyne ion trap, which are the same as those of the stretched ion trap used in the Finnigan ITD and ITMS [15] and very close to those of the Varian Saturn (Varian Chromatography Systems, Walnut Creek, CA) series of ion traps. The traps have a $r_o = 1$ cm and $z_o = 7.83$ mm with hyperbolic profiles corresponding to $r_o = 1$ cm and $z_o = 7.07$ mm [15] (which result from the theoretical relationship $r_o^2 = 2z_o^2$). The end cap apertures were 1.2 mm in diameter, and a single hole end cap was used for both inlet and exit.

3.2. Collision model

The collision model was based on hard-sphere collision physics assuming the buffer gas was at rest relative to the ion. An annotated description of the SIMION user program that contains the collision model is given in Appendix A. Functionally, the probability of a collision occurring was exponentially dependent upon the distance travelled in a time step such that the average distance between collisions equaled the mfp. The angle of impact and radial position for each collision was determined via a random number and the transfer of momentum was computed assuming hard-sphere collision physics between the two atoms with the buffer gas at rest. The resulting three-dimensional velocity vectors for the ion were determined from the change in momentum and a randomly chosen angle of deflection.

To correlate the experimental measurements with the model, an mfp was calculated based on the measured pressure (corrected for gas composition) using the standard equation [18]:

$$\lambda = \frac{RT}{\pi d^2 N_A P \sqrt{2}} = \frac{kT}{\pi d^2 P \sqrt{2}} \quad (1)$$

where d was taken to be the hard-sphere diameter for the helium atoms ($d_{He} = 2.3$ Å [18]), P is the pressure, N_A is Avogadro's number, R is the gas constant, and

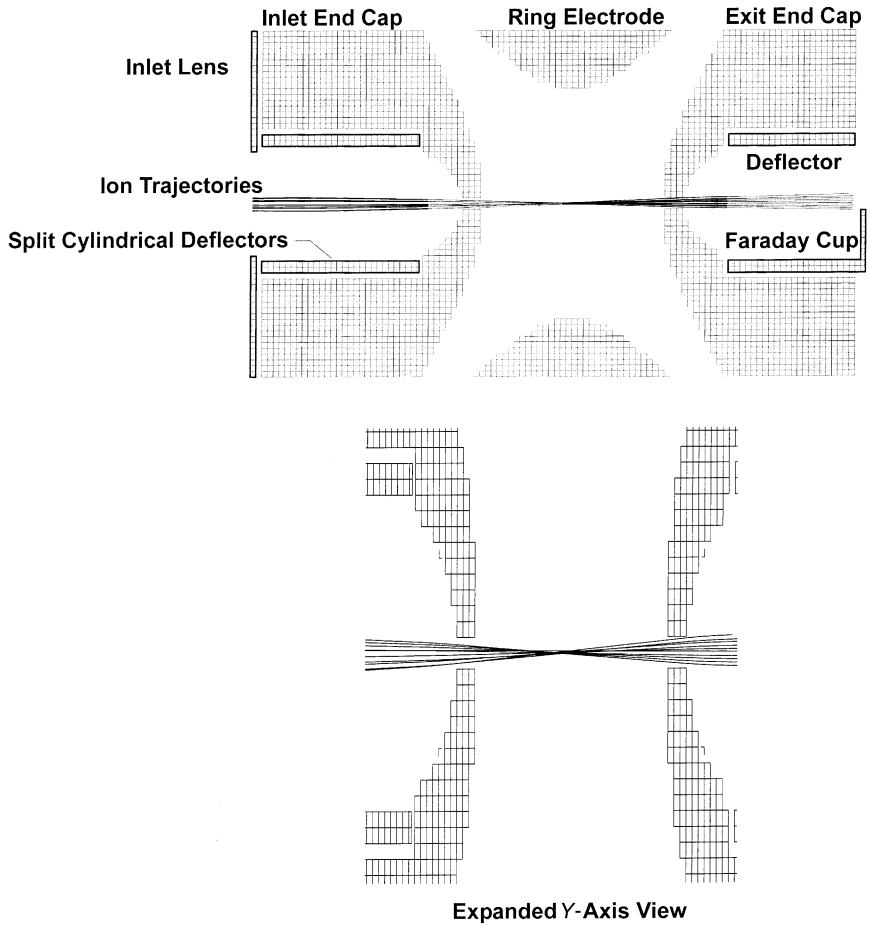

Fig. 2. A cross-section of the SIMION model of the ion trap and associated lenses and a set of ion trajectories for 12-eV ions (top). The inlet lens potential is −104 V, the cylindrical deflectors are at −12.4 V, and the end caps and ring electrode are at ground. The scale is 0.5 mm/gu. In the lower view, the *y*-scale is expanded to better illustrate the low divergence angle of the ion trajectories.

k is the Boltzmann constant. The pressure, *P*, was the calibrated gauge pressure corrected for the gas composition (0.18 for helium relative to 1.0 for nitrogen) [19,20]. The assumption of a static buffer gas is probably reasonable for the majority of the ion's trajectory through the ion gun and flight tube, where it is moving at ∼12 mm/μs, relative to the helium thermal velocity of ∼1 mm/μs. However, upon deceleration into the ion trap the velocity of the Cs^+ (∼3 mm/μs at 6 eV) and the helium are nearly equal, and the assumption of a static buffer gas may be incorrect. Further comments on the mfp calculation are contained in Section 5.

4. Results

4.1. Assessment of the collision model by comparison with experiment—collision gas pressure and ion energy effects

Initial experiments were conducted to verify that the collision model was qualitatively and quantitatively predictive. The ion trajectories were calculated along the entire beam line and into the ion trap with the collision model active. The voltages used in the simulation were the same as those used in the experiment,

with slight adjustments in the einzel lens and deflectors to compensate for the non-perfect alignment of the experimental system. The following procedure was applied in setting the voltages in the simulation. The voltages for the ion gun einzel lens, which controls the beam diameter, and the deflectors were adjusted in the simulation so that the ratio of the number of ions striking the inlet end cap (N_i) to the number of ions striking the exit end cap (N_e), and the ratio of the number of ions striking the inlet end cap to the number of ions striking the Faraday cup (N_{fc}) in the simulation matched (as closely as possible) these same ratios as measured in the experimental system. That is:

$$\frac{N_i}{N_e} \approx \frac{I_i}{I_e} \quad \text{and} \quad \frac{N_i}{N_{fc}} \approx \frac{I_i}{I_{fc}}$$

where I_i is the measured current at inlet end cap; I_e is the measured current at exit end cap; I_{fc} is the measured current at Faraday cup.

These measurements and simulations were performed at low helium pressure (1×10^{-6} Torr gauge) and with the rf voltage on the ring electrode at zero. Setting the lens voltages at low pressure ensured that the tuning was purely a function of the ion optics and did not include any collision effects, and helped to ensure that the characteristics (angular spread) of the simulated ion trajectories matched the experimental conditions. These beam-tuning settings were then held constant for all remaining simulations as the buffer gas pressure was increased; thus the changes in the ion trajectories were due solely to collision effects. To compare the measured currents to the predicted values at each of the three locations, the measured currents were normalized to the sum of the ion currents measured at the two end caps plus the Faraday cup, and the predicted values were normalized to the total number of ions that hit the two end caps plus the Faraday cup. A range of ion energies from 3 to 100 eV were tested and modeled. In the simulations, typically 100 sets of 1000 ions were flown at each pressure and averaged. Results for 6- and 12-eV ions are shown in Figs. 3 and 4, respectively.

At the longest mfp of ~1200 cm the ion beam is focused so that ~75% passes through the inlet end cap aperture. As the mfp is reduced, ions are scattered by collisions and the number hitting the inlet end cap

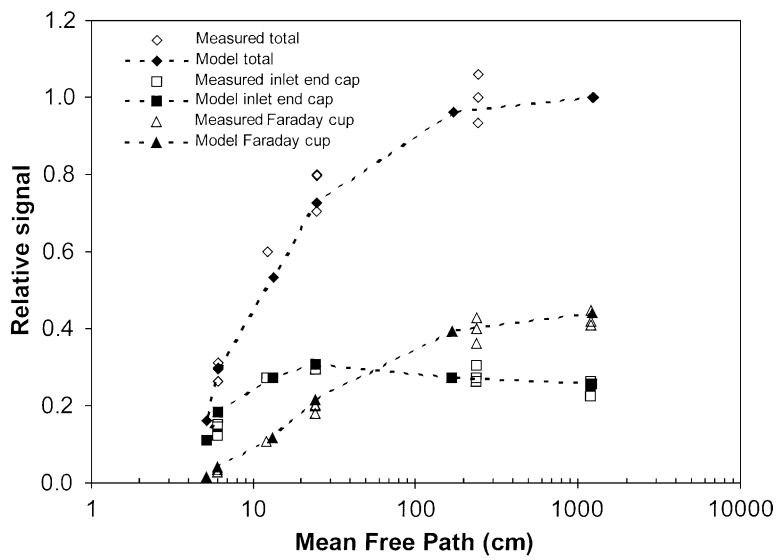

Fig. 3. Measured and predicted relative ion signal, normalized to the total, at the ion trap inlet end cap, at the Faraday cup, and the total (inlet and exit end caps plus Faraday cup) as a function of the mfp in helium buffer gas for Cs^+ ions with 6 eV of energy. The signal at the exit end cap is not shown for clarity.

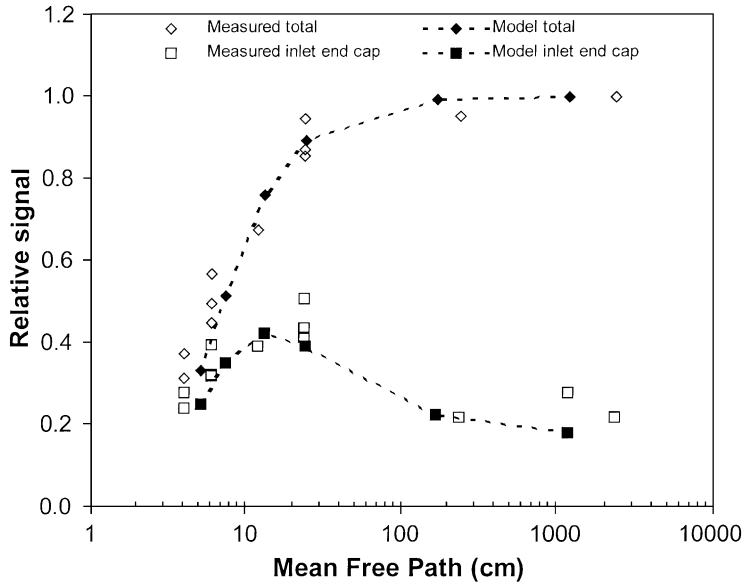

Fig. 4. Measured and predicted relative ion signal, normalized to the total, at the ion trap inlet end cap and the total (inlet and exit end caps plus Faraday cup) as a function of the mfp in helium buffer gas for Cs^+ ions with 12 eV of energy. The signal at the exit and cap and Faraday cup are not shown for clarity.

increases as the number passing through (Faraday cup signal) decreases. As the mfp approaches ~20 cm the inlet signal stops increasing. This occurs because the collisional scattering is severe enough to deflect the ions into the flight tube or inlet lens walls, reducing the total number that make it to the inlet end cap. The fact that the collision model predicted this in such good agreement with the experiment, indicated that both the collision and the geometrical models accurately represented the physical system. This behavior was observed at both low (6 and 12 eV) and high (68 and 100 eV, not shown) ion energies.

4.2. Geometrically sensitive resonance effects (q_z) on ion trapping

It is known and has been shown [7] that the amplitude of the ring electrode rf potential has an effect on the efficiency of trapping ions injected from outside the ion trap, and that the effect is dependent upon the ion energy and mass. Indeed, for pulsed injection (as opposed to continuous beam injection used in these studies) this phenomenon can be used to optimize trapping efficiency [2,3]. To test the predictive capability of the model for these known effects of ion trap geometry and operating conditions, measurements and simulations were performed to investigate the effect of the q_z value and the energy of the injected ion on the ion trapping efficiency. It was anticipated that since these experiments could be conducted with an atomic ion, thereby removing possible effects of molecular ions (primarily collision-induced dissociation during injection, cooling, or scan-out [21]), and for known and controlled energies, that examining the effect of q_z and ion energy on ion trapping would be a highly specific test of the fidelity of the geometric model (specifically the grid resolution in the simulation of the ion trap) and the collisional model (which includes energy-dependence in the collision physics). This is a very stringent test of the quality of the model because the resonance displayed in the efficiency versus q_z curve is dependent upon higher order fields within the ion trap, and the purity and magnitude of these fields is critically dependent upon the trap

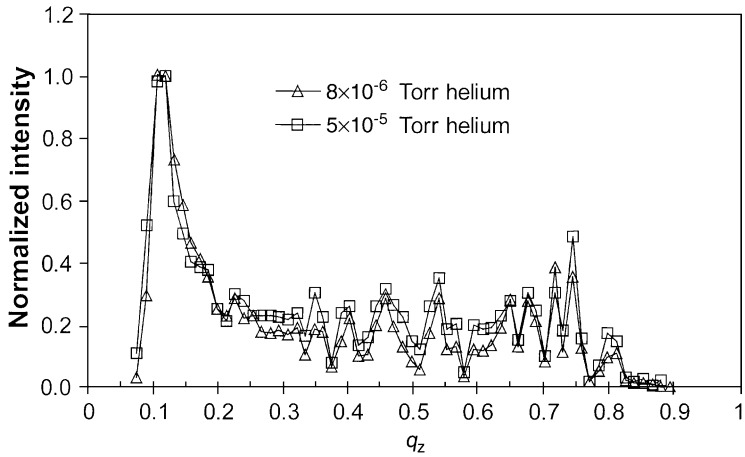

Fig. 5. Measured trapped ion signal normalized to the maximum at each pressure for 5-eV Cs^+ as a function of the operating level of the rf during trapping at two helium buffer gas pressures.

geometry (and implicitly the model resolution). Fig. 5 shows the experimental results for the dependence of ion trapping on the q_z value, in this case measured for 5-eV Cs^+ at two different helium pressures. Note that there is very little effect of pressure (over this range), and that there are multiple peaks and valleys in the signal.

The effect of ion energy is shown in Fig. 6, in which the q_z range, that includes the highest signal for each energy, is plotted for three different injection energies. There is a shift in the position of the maximum from a q_z of 0.14 to a q_z of 0.26 in going from 6.5 to 24 eV injection energy, respectively. This behavior had been suggested previously [7], and for injection of ions with a broad energy range results in a very broad peak at the low q_z values. In the present case, the energy distribution of the Cs^+ ions is relatively narrow and well-controlled. The dependence on ion kinetic energy was viewed as a good case for testing the simulation model.

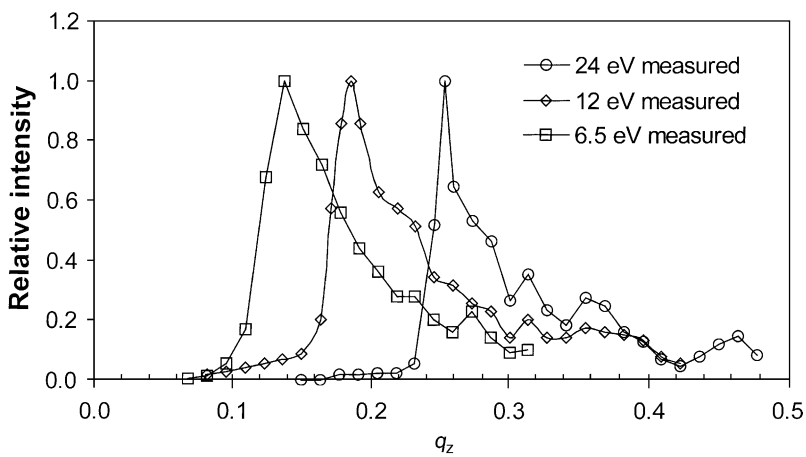

Fig. 6. Measured trapped Cs^+ ion signal normalized to the maximum at each energy for three injection energies as a function of the rf level during trapping at 1×10^{-4} Torr helium.

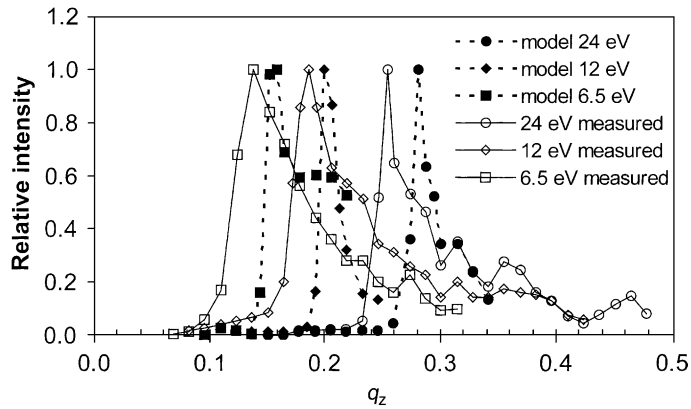

Fig. 7. Measured and predicted trapped Cs^+ ion intensity normalized to the maximum intensity at each energy for three injection energies as a function of rf operating level at 1×10^{-4} Torr helium.

Fig. 7 shows the measured results compared to the model. There is a clear and consistent offset, the model predicting the peak at slightly higher q_z values than the measured results. Several sources for the offset were considered: beam energy skewing, pressure effects, rf, and model resolution. These simulations were performed with an ion trap geometrical resolution of 0.5 mm/gu.

There could be a discrepancy in the actual beam energy (the offset corresponds to the equivalent of a 3 eV energy offset). This could be due either to error in the measured beam energy (at the trap inlet), or an error in the average beam energy in the model (again, at the trap inlet), perhaps due to the collision model. The beam energy in the experiment was measured using a blocking voltage method and the distributions were quite narrow (0.75 and 1.2 eV FWHM for the 6.5 and 24 eV energies, respectively, at 1×10^{-4} Torr helium) and the peak in the energy distribution corresponded to the assumed beam energy (based on the ion gun settings) to within 0.5 V (see Fig. 8). The ion energies for those ions that were trapped in the simulation were recorded as they entered the trap (corresponding to the blocking voltage location in the measurements).

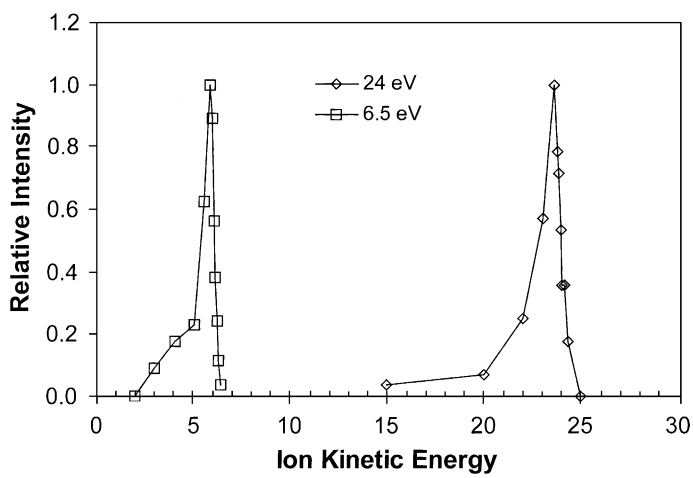

Fig. 8. Measured kinetic energy distribution of the 6.5- and 24-eV ions at the ion trap entrance end cap with 1×10^{-4} Torr helium buffer gas.

This also showed that there was very little skewing of the energy distribution, consistent with the fact that in a collision between a 4 and 133 amu particle there is very little loss of energy (∼5.7%) by the 133 amu particle. Thus, both of these possible errors were discounted. The effect of pressure was negligible and not considered adequate to explain this difference. Another factor that could effect this is the frequency of the rf potential. This was measured with a digital oscilloscope and the simulations were performed with the measured rf (which was different by ∼1 kHz from the value displayed in the data system); again the change was too small to account for the differences.

The final suspect was the geometrical resolution of the trap model in the simulation. The ion trap model being applied had a resolution of 0.5 mm/gu, and was a three-dimensional model. In order to investigate the sensitivity of the model to the geometrical resolution, the trap model was converted to a two-dimensional cylindrical model and three different geometrical resolutions were tested, the original (0.5 mm/gu) along with models with four and eight times higher resolution. The results are shown in Fig. 9 for ions injected with 24 eV kinetic energy; the 8× model predicts the measured result best. Fig. 10 shows the predictions with the 8× model and the measured results for three injection energies. In all three cases, the predictions are in excellent agreement with the data. It was thus concluded that the offset observed with the original model (using 0.5-mm/gu resolution) resulted from the slight differences in the rf field that in turn resulted from the lower resolution. The agreement with the 8× model (0.0625 mm/gu) indicates sufficient resolution within the model. This is consistent with the results of a comparison between different simulation models which showed that a resolution of 0.0444 mm/gu adequately predicted trap performance compared to analytical models [22]. The 8× model was incorporated into the full system simulation and all of the trapping efficiency predictions were performed with the 8× model.

4.3. Trapping efficiency

The quantitative trapping efficiency was determined by measuring the total ion current injected into the ion trap (ions passing through the inlet end cap aperture with the ring rf turned off and the inlet end cap grounded) and the integrated ion current ejected from the ion trap after trapping ions for a set period. Trapping was performed at several different q_z values for Cs^+ ($m/z = 133$) for times ranging from 5 to 15 ms. A cooling time of 300–500 ms was used between the end

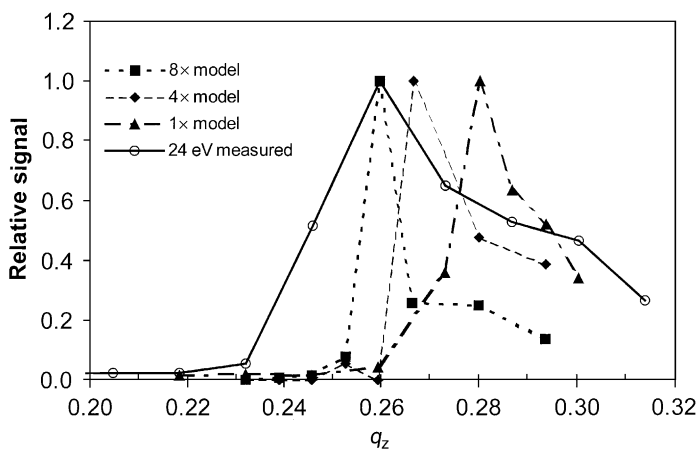

Fig. 9. Predicted trapped ion signal as a function of q_z for three different model resolutions and the measured response for 24-eV Cs^+ ions normalized to the maximum for each. The 1× model resolution is 0.5 mm/gu, the 8× model is 0.0625 mm/gu; helium pressure of 1×10^{-4} Torr for all cases.

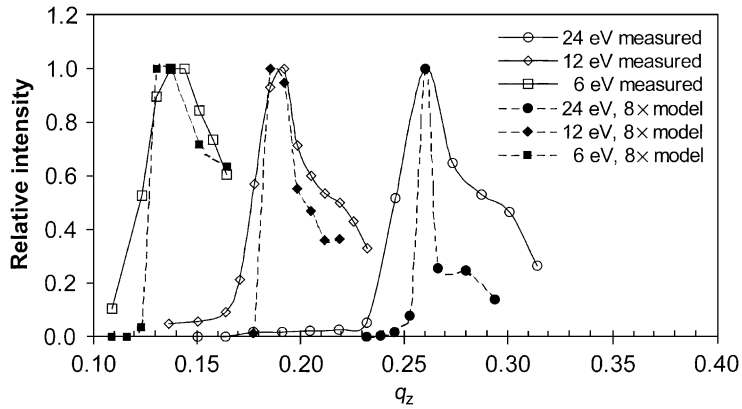

Fig. 10. Measured and predicted trapped ion signal normalized to the maximum for three different injection energies using the 8× resolution model; helium pressure of 1×10^{-4} Torr for all cases.

of the trapping period and the initiation of the scan-out in order to ensure that the trapped ions had adequate time to lose kinetic energy and collect at the center of the trap so they would pass through the exit end cap aperture upon ejection. While this cooling time is uncharacteristically long relative to "typical" operation, it was experimentally determined to be necessary at the low buffer gas pressures ($<5 \times 10^{-5}$ Torr). The need for the long cooling time is consistent with the fact that the exit end cap had only a single aperture (most commercial ion traps have an exit end cap with seven apertures), necessitating that the ions be cooled to the very center of the trap before ejection; and at lower pressures the collision rate is slow, necessitating a longer time to ensure that the ions are cooled to the center of the trap. It was also experimentally determined that there were no significant losses of ions during this extended cooling time.

The ions were scanned-out of the trap using the standard axial modulation resonance ejection method and the peak area for the Cs^+ was converted into equivalent current for determining the ratio of injected current to trapped current. During scan-out the inlet end cap lenses were at relatively low potentials (<15 V) and there was no detectable effect of the inlet end cap lens potential at these low voltages on the ejected ion signal. Thus, in the efficiency calculations, the measured signal was assumed to represent half of the trapped ions, the other half being ejected out the inlet end cap.

Trapping simulations were carried out with the full model of the instrument using the 8× (0.0625 mm/gu) ion trap model geometry and the collision model previously described. In the trapping simulations typically 50,000 to 100,000 ions were flown for a particular level of helium pressure, each ion was initiated at a random angle (±15°) and time (relative to the phase of the rf), and delta position (±0.8 mm) at the ion source in the ion gun. The sets (50–100 or more) of 1000 ions were flown at each set of conditions and the trapping efficiency was calculated for each set. The efficiencies for the sets were then averaged in order to get an estimate of the variance in the simulation for comparison with the variance in the measurements. The voltages on the ion gun and the remainder of the ion optics train were set to those used in the measured experiments, with slight adjustments to account for misalignment of the experimental system and uncertainty in the initial conditions for the ions at the ion source. The actual angular and positional spread of the emitted ions are parameters that we cannot measure, and so these adjustments enabled the ratio of the number of ions hitting the inlet end cap to those hitting the exit end cap and Faraday cup in the simulation to be matched to the measured ratio. This was used as an indication that the ion initial conditions and beam focusing in the simulation were properly representing the experiment.

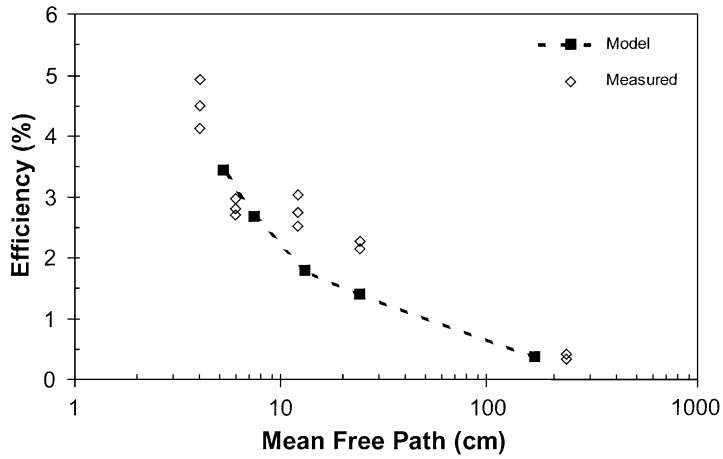

Fig. 11. Measured and predicted trapping efficiency for 6.5-eV Cs^+ in helium as a function of the mfp in helium at q_z of 0.13.

Measurements and simulations were conducted over a range of ion energies as a function of helium pressure (mfp) and at a variety of q_z values. The measured pressure (taking into account the gas correction factor and the ion gauge calibration factor) was converted to an equivalent mfp using Eq. (1) in order to compare the measured data against the simulation results. Fig. 11 shows the results for 6.5-eV ions. The agreement is relatively good, the model perhaps under-predicting the measurements slightly. Fig. 12 shows the results for 12-eV ions at two different q_z values. In this case, the simulation predicts slightly higher values than the measured at the "optimum" q_z of 0.18 (optimum being the q_z at which the maximum occurs in Fig. 10), while at a q_z of 0.21, the predicted values are closer to the measurements. Fig. 13 shows the results for 24-eV ions at a q_z of 0.26; in this case, the agreement is very good. The cause of the larger difference between predicted and measured for the 12-eV ions at $q_z = 0.18$ is not known, but the same trend was anecdotally observed in many other measurements for the 12-eV ions. One can conjecture that

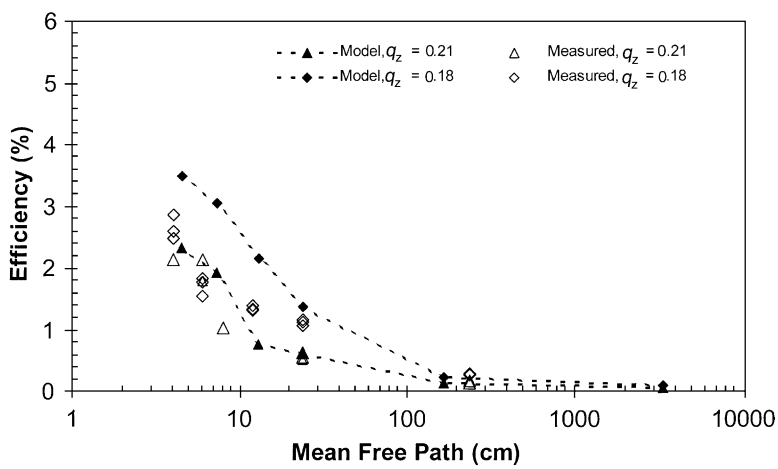

Fig. 12. Measured and predicted trapping efficiency for 12-eV Cs^+ in helium as a function of the mfp in helium at q_z of 0.18 and 0.21.

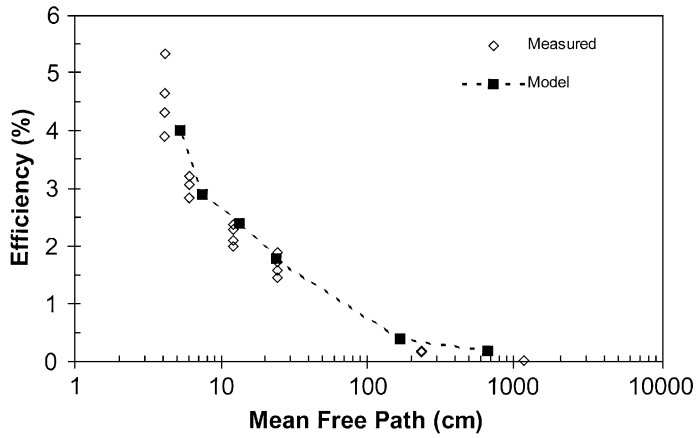

Fig. 13. Measured and predicted trapping efficiency for 24-eV Cs^+ in helium as a function of the mfp in helium at q_z of 0.26.

there was some particular aspect of the ion beam focusing at the 12-eV settings in the experiment that resulted in ion trajectories that were less optimum for trapping. Note that at the "optimum" q_z conditions, the measured trapping efficiency for the 12-eV ions at an mfp of 4 cm (~2.6%) is lower than the measured efficiency at both 6 and 24 eV (~4.5%). In all of the simulations, the variance about the average efficiency for mfps <20 cm was in the order of 60%, while the standard deviation for the measurements was lower, in the order of 30%. The measured and predicted efficiencies seen in Fig. 12 for 12-eV ions agree within these uncertainty ranges. In summary, we found that the simulation was able to predict the efficiency of trapping within the uncertainties of the measurement and calculations, and that the observed dependence of trapping efficiency upon q_z, buffer gas pressure, and ion kinetic energy are consistent with known performance characteristics of the ion trap.

5. Discussion and Conclusions

The simple hard-sphere collision model applied to the range of pressures and operating conditions of the ion trap mass spectrometer tested, appears to be sufficiently robust to predict not only the qualitative but also, within the uncertainty bands of the measurements and predictions, the quantitative performance of the system. The success of the model in predicting the absolute efficiency of trapping was surprising, perhaps fortuitous, given the number of parameters that are involved and the simplicity of the collision model. A primary example is the calculation of the mfp. The calculation includes the effect of the collision cross-section (πd^2) assumed for the buffer gas, the calibration of the pressure gauge, and the correction for gas composition, all of which include uncertainties of 30% or more. The values for the atomic diameter d used in this study were chosen based on what appeared to be the most relevant data available in the literature, but for example suggested values ranged from 1.9 to 2.3 Å for helium [18]. The uncertainty of the collision cross-section could be reduced by calculating an effective cross-section using the measurements of the loss of beam intensity with increasing pressure, and this has been performed by others for large molecular ions [23]. We chose not to apply this approach in keeping with the goal of using a relatively simple model with "best known" values for such variables. This conclusion is not intended to be a sweeping acclamation of the simple hard-sphere collision model, but merely an observation that under the somewhat constrained and narrow conditions tested, it performed at a level that gives us confidence in applying it for evaluating alternate geometries and operating conditions for

ion injection and trapping with helium buffer gas. For higher mass buffer gases, or at higher buffer gas temperatures, the transfer of energy from a moving buffer gas atom/molecule to the ion could be significant and should probably be incorporated into the model. With respect to the collision cross-section, if a more realistic momentum transfer calculation is applied (to account for grazing angle collisions) then a collision cross-section, that takes into account the diameters of the colliding particles, should probably be applied.

A particular caution that this study illustrates is the need to match the fidelity of the geometric models to the required predictive need. In this case, the ion trap model was of sufficient resolution at 0.5 mm/gu to predict the general dependence on variables such as the pressure and ion energy. Indeed, trapping efficiency simulations with the 0.5-mm/gu model (data not shown) were essentially the same as those predicted with the 0.0625-mm/gu model. However, when subtle effects like the sensitivity of the trapping efficiency to the rf level during trapping at low q_z values was investigated there was a bias introduced by the coarseness of the resolution in the 0.5-mm/gu model. The bias was removed when the higher resolution model (0.0625 mm/gu) was applied. This is yet another example of the need to heed the cautionary statement in the SIMION manual with regards to simulations: "Always be suspicious!"

The absolute value of the measured trapping efficiencies (∼5%) are consistent with previous estimates, based on modeling [7,11] and on "system" efficiencies [4], and demonstrate that only a relatively small fraction of the ions are actually trapped during continuous beam injection. The effect of the buffer gas pressure is pronounced, and indicates that for ions with masses in the 100 amu range and helium buffer gas, collisions with the buffer gas are important in the trapping process. For much higher mass ions it has been proposed that the buffer gas may play a less important role since the energy loss in a collision decreases as the ion mass increases [3].

In the course of these studies, anecdotal observations lead us to believe that there are ways to increase the trapping efficiency for continuous injection (as opposed to pulsed injection [3,24]), beyond the obvious method of using as high a buffer gas pressure as possible. In particular, the trapping efficiency seemed sensitive to the angle of injection of the ions into the trap. We are investigating this by using an end cap with a large aperture covered with a coarse grid and injection optics that cause the ions to diverge as they enter the trap.

Acknowledgements

The authors acknowledge M.B. Ward for valuable assistance in the mechanical design and fabrication of many of the instrument components, and the reviewers for their careful and thoughtful critique. Research supported by the DOE under contract with BBWI (DE-AC07-99ID13727).

Appendix A. Annotated SIMION user program for collisional cooling

```
; ---------- collisional cooling simulation ----------

                                ; get mean free path (mfp) and convert to polar coordinates

rcl mean_free_path_mm           ; get mean free path for one visible atom
rcl ion_vz_mm                   ; get the ion velocity
rcl ion_vy_mm                   ; load velocity vectors
rcl ion_vx_mm
>p3d                            ; convert velocity to polar coords
sto v                           ; save in temporary variables
rlup sto az
rlup sto el
```

Appendix A (*Continued*)

```
                                ; test for collision

rcl v rcl ion_time_step *       ; compute distance ion will travel in this time step from tstep * v
rcl mean_free_path_mm / chs e^x ; calculate the exp ratio of the distance and the mfp (1-e(-d/fp))
1 x<>y -                        ; this increases probability of collision as traveled distance approaches mfp
rand                            ; get a random number from 0 - 1
x>y goto skip1                  ; compare to the exp ratio, if rand is less than ratio then a
                                ; collision occurs; if not, a collision does not occur so skip collision calculation

                                ;collision occurs, determine impact angle

                                ; collision -- assume a variable
                                ; position hit on resting gas molecule, get a random radius r
1 rand x>=y goto skip1          ; no collision if r >= 1.0, jump to skip1
abs x>0 sqrt                    ;check the random number is >0 then take square root of number to force
                                ;equal area probability r value
                                ;convert the collision radius to an angle in radians
asin                            ;collision angle in radians
sto impact_angle_rad            ; save in local variable

                                ; assume direct hit on resting gas molecule, calculate attenuated velocity

rcl ion_mass rcl collision_gas_mass -   ;calculate the transfer of momentum assuming helium collision
rcl ion_mass rcl collision_gas_mass + / ; (m - 4)/(m + 4)
x=0 0.000001                    ; protect against identical mass blowup, if x=0 then make it 0.0000001
rcl v * rcl impact_angle_rad cos * sto vr   ; calculate attenuated radial velocity
rcl v rcl impact_angle_rad sin * sto vt     ; calculate attenuated tangential velocity
rcl vr rcl vr * rcl vt rcl vt * + sqrt sto v ; compute resulting velocity

                                ; calculate resulting angle of deflection and convert back to rectilinear coordinates

rcl impact_angle_rad rcl vt rcl vr / atan -
>deg                            ; calculate elevation off of vertical
90 +                            ; rotate 90 degrees and
360 rand *                      ; randomly choose an azimuth angle
rcl v                           ; recall velocity, convert angle and speed to rectilinear coordinates
>r3d                            ; compute rectilinear assuming vertical is on original line
-90 >elr                        ; el rotate back from 90 vertical
rcl el >elr                     ; el rotate to initial el
rcl az >azr                     ; az rotate to initial az
sto ion_vx_mm                   ; store new velocity vectors back into user variables
rlup sto ion_vy_mm
rlup sto ion_vz_mm              ; ion now has a modified velocity and direction
```

References

[1] R.R. Vargas, R.A Yost, in: R.E. March, J.F.J. Todd (Eds.), Practical Aspects of Ion Trap Mass Spectrometry, vol. 2, CRC Press, New York, 1995, p. 217.

[2] J. Qin, B.T. Chait, Anal Chem. 68 (1996) 2102.

[3] V.M. Doroshenko, R.J. Cotter, J. Mass. Spectrom. 32 (1997) 602.

[4] P. Kofel, in: R.E. March, J.F.J. Todd (Eds.), Practical Aspects of Ion Trap Mass Spectrometry, vol. 2, CRC Press, New York, 1995, p. 51.

[5] V. Steiner, C. Beaugrand, P. Liere, J.C. Tabet, J. Mass Spectrom. 34 (1999) 511.

[6] J.C. Schwartz, R.G. Cooks, M. Weber-Grabau, P.E. Kelley, in: Proceedings of the Thirty-sixth ASMS Conference, San Fransisco, CA, June 1988, pp. 634.

[7] S.T. Quarmby, R.A. Yost, Int. J. Mass Spectrom. 190/191 (1999) 81.
[8] S.A. McLuckey, G.L. Glish, K.G. Asano, B.C. Grant, Anal. Chem. 60 (1988) 2220.
[9] R.E. Kaiser Jr., J.N. Louris, J.W. Amy, R.G. Cooks, Rapid Commun. Mass Spectrom. 4 (1989) 225.
[10] J.D. Williams, H.P. Reiser, R.E. Kaiser Jr., R.G. Cooks, Int. J. Mass Spectrom. Ion Processes 108 (1991) 199.
[11] C. Weil, M. Nappi, C.C. Cleven, H. Wollnik, R.G. Cooks, Rapid Commun. Mass Spectrom. 10 (1998) 742.
[12] J.M. Wells, W.R. Plass, G.E. Patterson, Z. Ouyang, E.R. Badman, R.G. Cooks, Anal. Chem. 71 (1999) 3405.
[13] L. He, D.M. Lubman, Rapid Commun. Mass Spectrom. 11 (1997) 1467.
[14] D.A. Dahl, Int. J. Mass Spectrom. 200 (2000) 3.
[15] J.E.P. Syka, in: R.E. March, J.F.J. Todd (Eds.), Practical Aspects of Ion Trap Mass Spectrometry, vol. 1, CRC Press, New York, 1995, p. 202.
[16] D.A. Dahl, A.D. Appelhans, M.B. Ward, Int. J. Mass Spectrom. Ion Processes 189 (1999) 39.
[17] D.A. Dahl, A.D. Appelhans, M.B. Ward, Int. J. Mass Spectrom. Ion Processes 189 (1999) 47.
[18] (a) J.O. Hirschfelder, D.F. Curtiss, R.B. Bird, Molecular Theory of Gases and Liquids, John Wiley & Sons, New York, 1954.;
(b) D.R. Lide (Ed.), Handbook of Chemistry and Physics, seventy-fourth ed., CRC Press, Boca Raton, 1993.
[19] J.E. Bartmess, R.M. Georgiadis, Vacuum 33 (1983) 149.
[20] Varian EYESYS Instruction Manual 6999-08-205, December 1998.
[21] J.E. McClellan, J.P. Murphy III, J.J. Mulholland, R.A. Yost, Anal. Chem. 74 (2002) 402.
[22] M.W. Forbes, M. Sharifi, T. Croley, Z. Lausevic, R.E. March, J. Mass Spectrom. 34 (1999) 1219.
[23] S.G. Roussis, J. Am. Soc. Mass Spectrom. 6 (1995) 803.
[24] G. Savard, Nucl. Instrum. Methods Phys. Res. B 126 (1997) 361.